On-line implementation of model free controller for oxygen stoichiometry and pressure difference control of polymer electrolyte fuel cell

Meziane Ait-Ziane, Marie-Cecile Pera, Cédric Join, Michel Benne, Jean-Pierre Chabriat, Nadia Yousfi-Steiner, Cédric Damour

Graphical Abstract

On-line implementation of Model free controller for oxygen stoichiometry and pressure difference control of polymer electrolyte fuel cell

M. Ait Ziane, M.C Pera, C. Join, M. Benne, J.P Chabriat, N. Yousfi Steiner, C. Damour

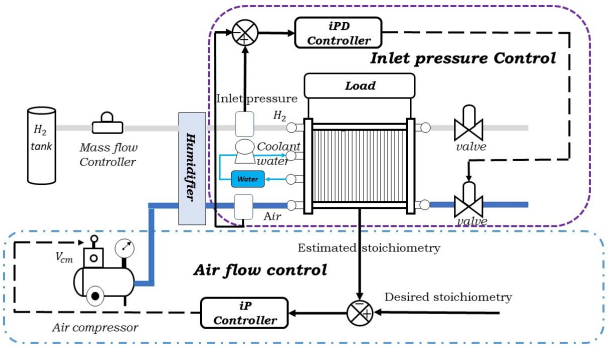

Highlights

On-line implementation of Model free controller for oxygen stoichiometry and pressure difference control of polymer electrolyte fuel cell

M. Ait Ziane, M.C Pera, C. Join, M. Benne, J.P Chabriat, N. Yousfi Steiner, C. Damour

- iP and iPD controllers have shown good performance in controlling oxygen stoichiometry and inlet pressure difference.
- The experimental validation showed a great ability to reduce the inlet pressure difference for different cases studied.
- The proposed controller offers better performance than the embedded industrial controller and can easily replace it.

On-line implementation of Model free controller for oxygen stoichiometry and pressure difference control of polymer electrolyte fuel cell

M. Ait Ziane[a,b], M.C Pera[b], C. Join[c], M. Benne[a], J.P Chabriat[a], N. Yousfi Steiner[b], C. Damour[a]

[a]*ENERGY Lab, Univ.La Reunion, rue cassin, Saint-Denis, 97715, France*
[b]*FEMTO-ST instiute, FCLAB, Univ.Bourgogne Franche-Comte,CNRS, rue Thierry-Mieg, Belfort, 90010, France*
[c]*CRAN,(CNRS,UMR 7039), Univ.Lorraine BP 239, Vandoeuvre-les-Nancy, 54506, France*

Abstract

This paper proposes and validates a model free controller to improve the real time operating conditions of Proton Exchange Membrane Fuel Cells (PEMFC). This approach is based on an ultra-local model that does not depend on a precise knowledge of the system. It is perfectly adapted to a complex system such as the fuel cell, while benefiting from the ease of online implementation and low computational cost. The designed controller is used to regulate both the oxygen stoichiometry and the membrane inlet pressure, which are crucial operating conditions for the fuel cell's lifetime. The objectives of the proposed control strategy are twofold: preventing the starvation failure, and limiting the potential for mechanical degradation of the membrane during a large pressure difference. The performance of the proposed control strategy is initially evaluated by a simulation environment for both oxygen stoichiometry and inlet pressure difference control of fuel cell stack. An online validation on 1.2KW fuel cell stack is conducted to control the membrane pressure drop. Two case studies are comprehensively investigated in relation to stoichiometry control: set point tracking and rejection of unmeasured disturbances caused by current variations. Simulations and experimental results reveal that the proposed controller provides significantly better performance in terms of fast trajectory tracking, and ensures less overshoot compared to the Fuzzy PID and PID controller. This efficiency is proven using the Integral Absolute Error (IAE), Integral Squared Error (ISE) and Integral of the Square input (ISU) performance indexes.

Keywords: Proton Exchange Membrane Fuel Cell (PEMFC), Intelligent proportional controller, On-line control, Oxygen Stoichiometry, Pressure difference

control.

1. Introduction

One of the major global environmental challenges is to reduce green house gas emissions, and dependence on fossil fuels. The convergence towards green and clean energy is imperative to meet this challenge. Polymer Electrolyte Membrane Fuel Cell (PEMFC) technology is one of the key technologies to achieve this goal. Among the advantages of this technology, providing simultaneously electrical and thermal energy. However, a PEMFC is a multiphysics system whose components are highly exposed to the risk of degradation, which results in a too short life span. Control and monitoring of operating parameters are mandatory to maintain the performance and efficiency in optimal conditions. In [1] [2], authors concluded that four crucial operating parameters have a direct impact on performance, reliability and lifetime: stoichiometry ratio, PEM fuel cell temperature, relative humidity, and inlet gases pressure.

Firstly, gas stoichiometry is one of the important parameters due to its impact on electrochemical reactions and water management in PEM fuel cells. Too low oxygen stoichiometry leads to a drop in PEMFC voltage, and prevents the release of the produced water [3]. A large amount of water upstream of the electrodes tends to inhibit the diffusion of gas into catalyst layers and may cause starvation fault[4]. A high oxygen stoichiometry ensures proper operation of PEMFC, but results in an increase in compressor power that reduces the overall efficiency of PEMFC systems and could dry out the membrane [5]. Secondly, effective stack temperature control maintains better membrane hydration and increases the efficiency of PEM fuel cells[6][7]. Inefficient temperature control directly affects the water balance in the membrane and the electrodes. Highly variable water content permits the occurrence of flooding and drying faults that have significant impacts on performance and lifetime of PEMFCs [4] [8]. Thirdly, inadequate inlet relative humidity of reactants can unbalance the water content in the membrane and the electrodes[9]. For that, a quick adjustment of the relative humidity of the gases is required to maintain the maximum power output of PEM fuel cells[10]. Finally, inlet partial pressure control is essential to avoid mechanical degradation of the membrane due to the large pressure drop between cathode and anode sides. Most suppliers recommend keeping this pressure difference below a few hundred mbar[3].

In recent years, many studies have presented model-based control strategies that have been applied to PEM fuel cell systems. Most work is focused on controlling oxygen stoichiometry to enhance performance, and avoid starvation fault. To keep

the maximum power delivred by PEMFC, an optimal oxygen stoichiometry reference obtained from experimental tests is introdued in the control strategy of [11]. For the same purpose, an adaptive sliding mode observer near-optimal oxygen stoichiometry controller is applied to control the air supply. The objective of the control is to follow the optimal oxygen stoichiometry to optimize the net power produced by PEM fuel cell [12]. A Linear-Quadratic Regulator coupled with a feedforward controller is applied in simulation [13]. The purpose of the offered control strategy is to reduce the disturbance effect when the load changes and to maintain the stoichiometry at the desired value. The objective of the control in[14] is to reach the maximum power with a variable stoichiometry. The employed controller consists of three parts: a nonlinear controller, a feed forward controller, and a PID feedback controller. The result illustrates the ability of the proposed controller to adjust the oxygen stoichiometry faster than a PID controller when the load changes. An active disturbance rejection controller (ADRC) is used to control oxygen stoichiometry in [15]. A model of PEM fuel cell is identified offline and represented by a transfer function for simplicity. Compared to PI controller, the simulation result exhibits that the ADRC controller provides less overshoot, and reaches the desired value comparatively faster. In [16] the main objective of the control is to maintain the fuel cell temperature at 350K during load variations, and when the cooling capacity of the radiator is maximum. A constrained predictive control model is applied in the simulation, the result shows the ability of the controller to perform the assigned task. An adaptive controller is applied to regulate the stack temperature during start-up procedures and power changes [17]. The simulation results showed the high efficiency of the controller in keeping the stack outlet temperature on the desired trajectory for different current changes compared to the PI controller. To improve the control of the water content inside the membrane, a flatness approach is applied in [18]. The objective of the strategy is to control the membrane humidity by acting on the airflow mass. The simulation results showed the ability of the controller to maintain the desired water in the presence of disturbances and uncertainties.
In [19], a second order sliding mode controller is applied in simulation to robustly regulate the relative humidity of the input gases taking into account internal and external disturbances. Furthermore, the model-based approaches are also tested experimentally. The control task in [20] is to stabilize the oxygen stoichiometry under disturbances and measurements noise. For this purpose, an adaptive sliding mode controller based on high order sliding mode observer (HOSM) is evaluated in simulation and in a real-time emulator. The results show that the proposed controller provides better convergence and robustness when the load varies compared to PID and sliding mode controller. A self-tuning PID strategy based on an artificial neural

network (ANN) is applied to a single PEM fuel cell in real time [21]. The ANN model identification is performed using offline training data, which can predict the oxygen stoichiometry of a 50W single cell. The experimental results show the potential of the controller to maintain stable stoichiometry by anticipating current changes. In order to minimize the inlet gas pressure difference to avoid membrane degradation, a robust nonlinear adaptive controller is used in [22]. An observer is designed to estimate system states, disturbances (known and unknown), and a sensor fault on the hydrogen inlet pressure measurement. Simulation results reveal that the proposed control strategy is able to maintain the hydrogen pressure close to the set point in the presence of uncertainties and sensor faults compared to the conventional PI and fuzzy controller. The designed observer exhibits satisfactory estimation errors in the majority of the studied cases. These errors are related to the dynamics of the observer which takes some time to estimate the disturbances that impact the system.

The approaches previously presented involve the modeling of fuel cell. However, this is not an easy task as a PEM fuel cell is a complex system to model due the coupling of electric, chemical, thermal, and fluid phenomena. Unmodeled system dynamics and external disturbances can be handled by designing a controller that does not depend heavily on the model. Fuzzy logic approaches have proven to be appropriate, and widely used to control different parameters in PEM fuel cell systems. In [23], a Direct Active Fuzzy Nonlinear controller is applied for pressure control in the simulation. The objective is to maintain the partial pressure of the supplied gases at 3 atm. The results demonstrate that the proposed controller ensures lower overshoot compared to nonlinear and PI controllers. A hybrid control strategy based on a self-adaptive PI controller is presented in [24], the gain tuning is provided by an advanced genetic algorithm and fuzzy logic. The main objective of the control is to ensure a small pressure difference at the PEMFC inlet during current changes. The controller is tested in simulation with a comparison to a non-linear controller. The results show that the given control architecture ensures half the pressure difference as the controller used as a reference. A dynamic model of a PEMFC for a mobile application oriented towards hydrogen inlet pressure control is presented in [25]. A self-adaptive PI controller is employed, the controller gains are updated with fuzzy logic. A feedforward controller is incorporated to improve the ability to reject disturbances. The disturbances are expressed as current change and system purge. Simulation tests showed a high ability of the controller to track the desired pressure and maintain the pressure under different current change and purge scenarios compared to the conventional PI controller and the fuzzy PI controller. An experimental validation on an 80Kw PEMFC is carried out, the results show that the control strategy is

able to maintain the pressure around the set point with an error of less than 2 KPa under a purge interval of 1.5s during the opening and 5s during the closing of the back pressure valve. To regulate oxygen stoichiometry, in [26] an adaptive controller based on Type-2 Fuzzy Logic Systems (T2FLS) is tested in simulation and experimentation. The results show that the T2FLS quickly tracks the desired value during setpoint, and load variations for different stack temperatures. Furthermore, a Fuzzy Logic controller is employed in [27] to control a cooling pump of a 5 kW PEM fuel cell system. The performance of the proposed controller is compared in simulation and experimentation to the PID and the state feedback controller. Fuzzy Logic proved to be faster in tracking the desired temperature without overshoot under different current variations. Moreover, the coupling of fuzzy logic and PID controller is presented in [28]: a feed-forward fuzzy associated with a fuzzy PID controller is used to regulate the oxygen stoichiometry. Additionally, the tuning of PID gains with fuzzy logic is presented in [29] to regulate oxygen stoichiometry. The simulation results show that the PID fuzzy controller provides better perforance than the feedforward PID controller for setpoint tracking.

Model-based control has shown considerable performance for various applications, but requires a deep knowledge of the modelled system which is not always easy to obtain. Fuzzy logic depends on the choice of interference rules and the type of membership functions, which makes the controller design more complex. Some of the methods presented above have a high computational cost that may sometimes require special equipment for real-time implementation.

To deal with the constraints and difficulties of obtaining the PEM fuel cell model, the computational cost of the controllers and their tuning complexity, a model-free controller, named an intelligent Proportional Integral Derivative controller ($iPID$) [30], is presented and tested in both simulation and experimentation in this paper. This approach is based on an ultra-local model that does not depend on the precise knowledge of the system. The main advantages of this approach are the online estimation of the dynamics of the controlled system only from the output measurement and the previous values of the control input with low computational cost [31]. On top of that, the satisfying results obtained in numerous studies for different applications [32] [33] [34] [35] motivated us to apply this approach to PEM fuel cell systems. Firstly, an iP and iPD are tested with a nonlinear model in the simulation to control both oxygen stoichiometry and inlet pressure difference. The objective of the simulation is twofold: the first one is to propose a fuel cell model allowing to control simultaneously the oxygen stoichiometry and the inlet pressure of the cathode. This model is assembled from different models found in the literature. The second is to test the performance of the proposed controller in simulation before applying it in

real applications with a comparison to controllers commonly used for real applications.
Secondly, experimental tests are performed on a PEM fuel cell stack of $1.2KW$ to validate the control of the membrane inlet pressure difference.

The organization of this paper is as follows: the second section summarizes the model-free control. The third and fourth sections present the simulation and experimental results, respectively. The conclusion and perspectives are given in the fifth section.

2. Model free approach

2.1. Model free control

Model-free control or Intelligent PID is introduced by C. Join and M. Fliess [30]. This strategy has proven good performances for the control of complex systems [36] supported by a low computational cost and an easy implementation in real time [37]. The principle of the model-free controller consists in replacing the precise mathematical model of the system by an ultra-local model defined by:

$$y^{(v)} = F + \alpha.u \tag{1}$$

Where:

- The output and the control variables are respectively y and u.
- (v) is the derivation order of output y (in practical case, (v) is often equal to 1 or 2)
- α is constant parameter to be defined, authors in [32] proposed a method to tune this parameter.
- F regroups the unmodeled part of the system and disturbances (the estimation of F is done via the input and output variables).

2.1.1. Estimation of F

The core of model free control is based on the estimation of F, which is approximated by a piecewise constant function F_{est} in a short period of time $[t - T; t]$. The dynamic of F is estimated from the previous input u and output y, using an algebraic numerical identification estimation technique [38] [39].
The *Laplace transform* is applied to the ultra-local model defined in Eq.(1) with $v = 1$:

$$sY(s) - y(0) = \frac{F}{s} + \alpha U(s) \tag{2}$$

Where F is approximated by a constant function, $Y(s)$ and $U(s)$ correspond to Laplace transforms of y and u respectively. Deriving both members to eliminate the initial condition $y(0)$:

$$Y(s) + s\frac{dY(s)}{ds} = -\frac{F}{s^2} + \alpha\frac{dU(s)}{ds} \tag{3}$$

The variable s refers to a derivative in the time domain. To avoid the risk of noise amplification by the derivative of a noisy signal, both members of the equation are multiplied by s^{-2}.

$$s^{-2}Y(s) + s^{-1}\frac{dY(s)}{ds} = -s^{-4}F + \alpha s^{-2}\frac{dU(s)}{ds} \tag{4}$$

The expression for F_{est} in time domain is deduced using the following correspondences between the frequency and time domains:

$$\begin{aligned} s^{-1} &= \int_0^t \\ s^{-n} &= \int_0^{(n)} \\ \frac{d}{ds} &= -t \\ \frac{dn}{ds} &= (-1)^n t^n \end{aligned}$$

Therefore,

$$F_{est} = \frac{-3!}{T^3}\left(\int^{(2)} y(t) - \int ty(t) + \int^{(2)} \alpha t u(t)\right) \tag{5}$$

The Cauchy formula Eq.(6) can be used to convert an iterated integral into a simple integral, which facilitates the implementation of such estimation algorithm.

$$\int_0^T \int_0^{t_1} .... \int_0^{t_{\gamma-1}} u(t_\gamma)dt_\gamma ...dt_1 = \int_0^T \frac{(T-t)^{\gamma-1}}{(\gamma-1)!}u(t)dt \tag{6}$$

Applying Eq.(6) in Eq.(5), we obtain:

$$F_{est} = \frac{-3!}{T^3}\int_{t-T}^{t} (T-2t)y(t) + \alpha t(T-t)u(t)\mathrm{d}t \tag{7}$$

Where $T > 0$ might be quite small and $[t-T;t]$ corresponds to the sliding windows of integration interval. The closed-loop control law in the case of iP controller is given by:

$$u(t) = \frac{1}{\alpha}\left(-F_{est} + \dot{y_d} + k_p e\right) \tag{8}$$

Where :

- y_d is the desired trajectory.
- $e = y_d - y$ is the tracking error.
- k_p is tuning gain of the controller proportional.

An ultra local model with $v = 2$ is required if an iPD controller is chosen. Eq.(1) becomes:

$$\ddot{y} = F + \alpha.u \tag{9}$$

In the same manner as before, *Laplace transform* is applied on Eq.(9):

$$s^2Y(s) - sy(0) - \dot{y}(0) = Fs^{-1} + \alpha U(s) \tag{10}$$

To eliminate the initial conditions, a derivative by $\frac{d}{ds}$ is applied:

$$2s^{-3}F = 2Y(s) + 4s\frac{dY(s)}{ds} + s^2\frac{d^2Y(s)}{ds^2} - \alpha\frac{d^2U(s)}{ds^2} \tag{11}$$

In order to mitigate the influence of noise on the measured output, we replace the derivative term by the integral function s^{-1} which has robustness properties against noise. Multiplying Eq.(11) by s^{-3} gives:

$$2s^{-6}F = 2s^{-3}Y(s) + 4s^{-2}\frac{dY(s)}{ds} + s^{-1}\frac{d^2Y(s)}{ds^2} - \alpha s^{-3}\frac{d^2U(s)}{ds^2} \tag{12}$$

The Eq.(12) can be written in time domain using elementary calculus and Cauchy's formula to simplify the multiple integral into a single one.

$$F_{est} = \frac{5!}{T^5}\int_{t-T}^{t}\left(T^2 + 6t^2 - 6Tt\right)y(t)\mathrm{d}t - \left(\frac{\alpha}{2}t^2(T-t)^2u(t)\right)\mathrm{d}t \tag{13}$$

The closed-loop control law in the case of iPD controller is given by:

$$u(t) = \frac{1}{\alpha}\left(-F_{est} + \ddot{y_d} + k_p e + k_d\dot{e}\right) \tag{14}$$

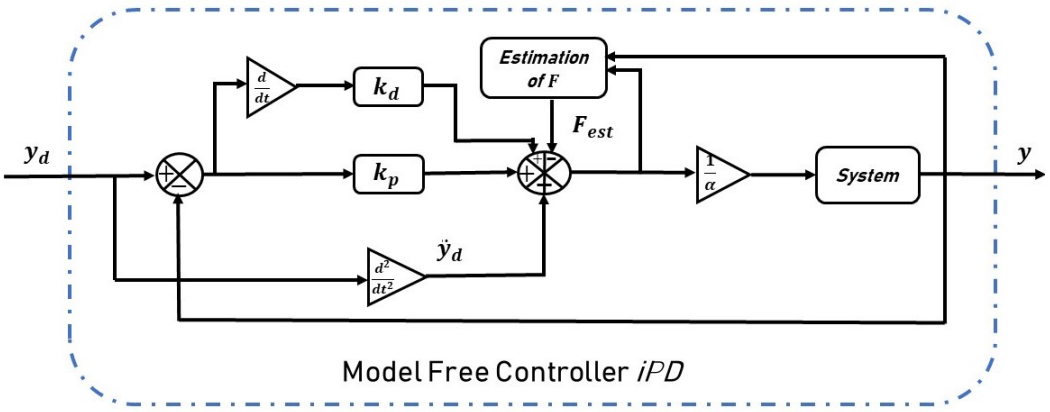

Figure 1: The diagram scheme of Model free controller iPD

Both of iP and iPD controllers are employed in this document, Fig.(1) illustrates the diagram of the closed-loop controller.
The choice of the output trajectory y_d is inspired from the flatness-based control rules [40]. The reference trajectory is not widely introduced in classical PIDs for industrial applications. This absence frequently leads to unwanted oscillations and control imperfections such as overshoot and undershoot [30].

2.2. Control objective

The control of the stoichiometry is important to maintain the correct functioning of the PEM fuel cells, which ensures the presence of the necessary amount of reactant during the electro-chemical reaction to avoid a starvation fault. The airflow rate can be considered as proportionnal to the compressor rotational speed, controlled through the rotation speed. Moreover, to avoid perforation and degradation of the membrane, keeping the gas inlet pressure balance is mandatory. In this paper, the simultaneous control of air stoichiometry and inlet pressure is addressed in simulation. The objective is twofold: maintaining the stichometry at a desired value while decreasing the pressure difference between the anode and cathode sides under different scenarios.
Experimentally, the test bench is fed by a bottle of pure oxygen and the flow rate is controlled through a mass flow controller, see section 4. The mathematical model of the 1.2KW PEM fuel cell and auxiliaries that are installed on the test bench is unknown. For this purpose, the validation of the proposed controller is an appropriate choice to control the inlet differential pressure.

3. Simulation results

The complete nonlinear fuel cell model used for the simulation is designed from three model elements found in the literature. The core of the PEMF fuel cell model is based on the work of [41]. However, to provide oxygen stoichiometry control, a compressor that supplies the PEM fuel cell with air flow is required. This model is deduced from the model found in [42]. In order to control the inlet pressure, a valve placed at the outlet gas of the stack is added which allows controlling either the outlet and/or the inlet pressure, this model is based on the work of [43]. The full model with the PEM fuel cell model parameters is presented in the Appendix. The sampling period for this part of the simulation is $2ms$. The model-free controller is benchmarked by comparing the performance obtained with a fuzzy PID and PID controllers in three case studies:

- Tracking oxygen stoichiometry while controlling the inlet pressure difference to 0.
- Maintain a fixed stoichiometry and inlet pressure difference when the load is varying, this variation is considered as a disturbance for the controller.
- Tracking the trajectory for the inlet pressure while maintaining the pressure difference at 0.

A white Gaussian noise of variance 0.02 is added to the output of oxygen stoichiometry. The air supply to the stack is provided by a compressor, the flow rate is regulated by controlling the compressor voltage. The inlet pressure is regulated by acting on the valve located at the outlet of the cathode side, the manipulated variable is the voltage which allows to control the opening and closing of the valve. The Fig.(2) shows the control scheme for the both control strategies.
The desired trajectory is obtained by filtering the setpoint according to the characteristics of a second order dynamics.

$$\frac{y_d}{E} = \frac{1}{(T's+1)^2} \tag{15}$$

Where: y_d is the desired trajectory, E refers to the setpoint and T' is a parameter allowing to fix the speed of the trajectory rise.

$$E = T'^2 s^2 y_d + 2T' s y_d + y_d \tag{16}$$

It can be discretized as follows:

$$s y_d = \frac{y_d(kT_s) - y_d(kT_s - T_s)}{T_s}$$

iP controller	iPD controller	PID for oxygen Stoichiometry	PID for inlet pressure difference
$\alpha = 0.5$; Kp= 9;	$\alpha = 5.10^{-}8$; $Kp = 25$; $Kd = 9$	$Kp = 400$; $Ki = 1000$; $Kd = 40$;	$Kp = 5.10^{-}6$; $Ki = 1.5.10^{-}5$; $Kd = 3.10^{-}7$;

Table 1: Gain values of the controllers

$$s^2 y_d = \frac{y_d(kT_s) - 2y_d(kT_s - T_s) + y_d(kT_s - 2T_s)}{T_s^2}$$

With $T' = \omega T_s$, we obtain:

$$y_d(kT_s) = \frac{y_d(kT_s - T_s)(2\omega + \omega^2) - y_d(kT_s - 2T_s)\omega^2 + E}{(1 + 2\omega + \omega^2)} \tag{17}$$

The trajectory is adjusted with the parameter ω, which determines the speed to reach the setpoint value. For this section of the paper, the iP controller is employed to control the oxygen stoichiometry, while the iPD is used to control the inlet pressure difference. For the control of oxygen stoichiometry, an iP controller has given acceptable performance, so a second order ultra-local model is not required. However, for the control of the inlet pressure, the dynamics of the system is fast and the architecture of the control is more complex, then an ultra-local model of order 2 is taken which leads to an iPD controller. The Table 1 shows the gain values of the controllers used in the simulation. The PID controller parameters are optimized with the Ziegler-Nichols method [44]. The design of a Fuzzy PID controller is done with two inputs to the fuzzy interface, the error e and $\dot{e}$. The outputs are the gains K_p, K_i and K_d of the PID controller. The fuzzy subsets and the basic form of the control rules are chosen as in [45].
It is important to notice that the PEMFC is operating in a current density region of less than 0.92 cm2, which does not result in any mass transfer limitation.

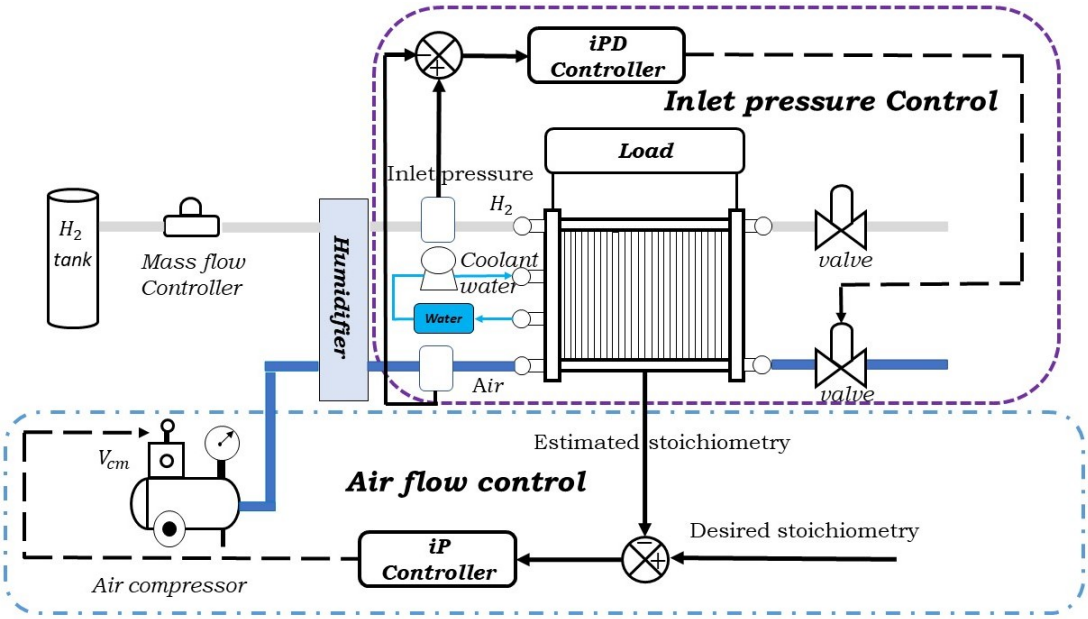

Figure 2: PEM fuel cell system control diagram

3.1. Stoichiometry trajectory tracking with reducing the inlet pressure difference

The aim of the control strategy is multiple: tracking the desired stoichiometry with a load fixed and keeping simultaneously the inlet cathode pressure at the same value of the anode inlet pressure. For oxygen stoichiometry control, the objective is to flow quickly the trajectory without any overshoot. Regarding the inlet pressure difference, the goal is to rapidly reduce this difference to 0 in order to preserve the membrane degradation as previously mentioned.

Stoichiometry setpoint tracking is performed at a fixed load of $180A$. An increase in oxygen stoichiometry from 2 to 3 is done at 2 seconds. Two decreasing steps in oxygen stoichiometry with an amplitude of 0.5 are applied successively at 4 and 6 seconds, as shown in Fig.3(a). The Fig.3(b) shows that the iP controller reaches the target faster than the Fuzzy PID and PID controllers in both cases of changing the desired trajectory. In addition to being slower, they offer an overshoot for all three setpoint changes. For inlet pressure control, the model-free controller employed is iPD. The variation of the oxygen stoichiometry implies a change of the inlet air flow which is relatively dependent on the inlet air pressure. Therefore, it is necessary to control the pressure in order to reduce the pressure difference between the anode and cathode side. The inlet pressure of the anode side is set at 3 barg, the objective is to regulate the inlet cathode pressure at the same value. The Fig.3(c) shows the variation of

the air inlet pressure during the various stoichiometry changes. The iPD controller offers a reduced inlet pressure difference compared to other controllers with a smooth adjustment to the anode inlet pressure. The fuzzy logic and PID controllers ensure a pressure difference greater than 0.3 barg for the first change of the stoichiometry as shown in Fig.3(d). For a real application with some PEM fuel cel stacks, this difference is very important and can cause significant damage to the membrane. The proposed controller achieved a pressure difference less than 0.25 barg for the first stoichiometry change and less than 0.15 barg for the other changes. It is interesting to note that the fuzzy logic PID performs better than the conventional PID for the first and second setpoint changes.

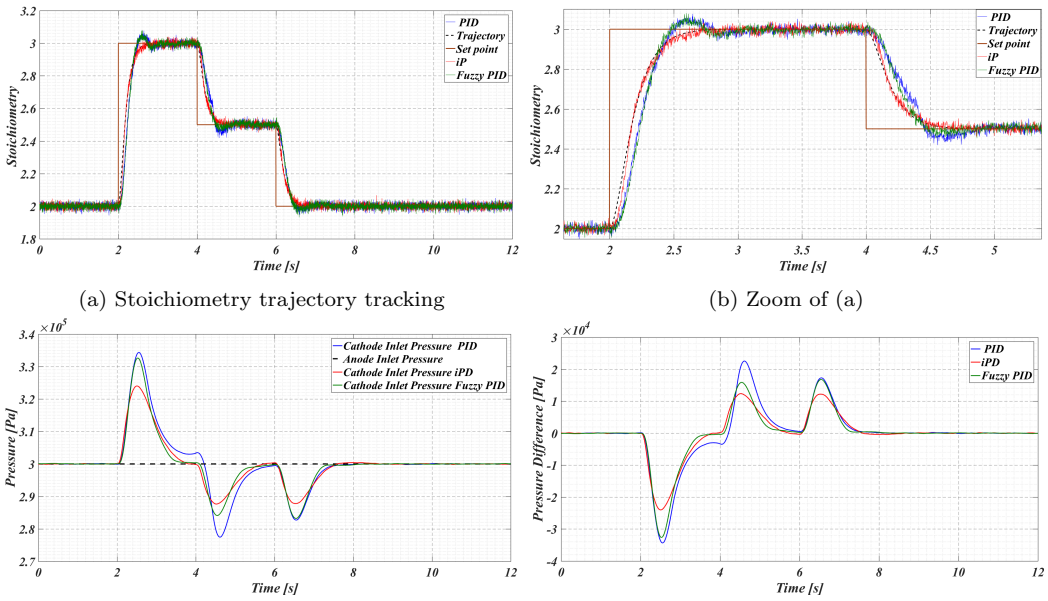

(a) Stoichiometry trajectory tracking

(b) Zoom of (a)

(c) Inlet pressure

(d) Inlet difference pressure ΔP

Figure 3: Stoichiometry trajectory tracking with reducing the inlet pressure difference

3.2. Disturbances rejection

The performance of the proposed controller is also tested for disturbance rejection as shown in Fig.4(a). The control objective is to maintain the oxygen stoichiometry at 2 under different load variation, as shown in Fig.4(b). The stack current increases from $180A$ to $200A$ at $1s$, from $200A$ to $230A$ at $3s$, from $230A$ to $250A$ at $5s$. A decrease from $250A$ to $240A$ at $7s$, additional decrease from $240A$ to $200A$ is carried out at $7s$, a reset to $180A$ is performed at $11s$. Fig4(a) shows the overall behavior of the controllers under variable load. It can be seen that the oxygen stoichiometry

is readjusted more rapidly with the iP controller. The second goal is to maintain the cathode inlet pressure at 3.2 barg, being the anode inlet pressure. Fig4(c) shows the behavior of the controlled air inlet pressure for different current variations. It is clearly observed that the iPD controller provides a fast fit with less difference between the two sides compared to Fuzzy PID and PID controllers, see Fig4(d). The proposed controller confirms that it provides less inlet pressure difference than other controllers when the airflow changes as shown in Fig4(e). This performance can be observed on the PEM feul cell voltage signal, Fig4(f). During current increases, the voltage supplied by the proposed controller increases rapidly compared to the fuzzy PID which is faster than the conventional PID. It is important to note that during current decay, the voltage of other controllers is better than that of the proposed controller, because the inlet air pressure is significant. This pressure has a direct impact on the voltage but also degrades the membrane which can shorten its life.

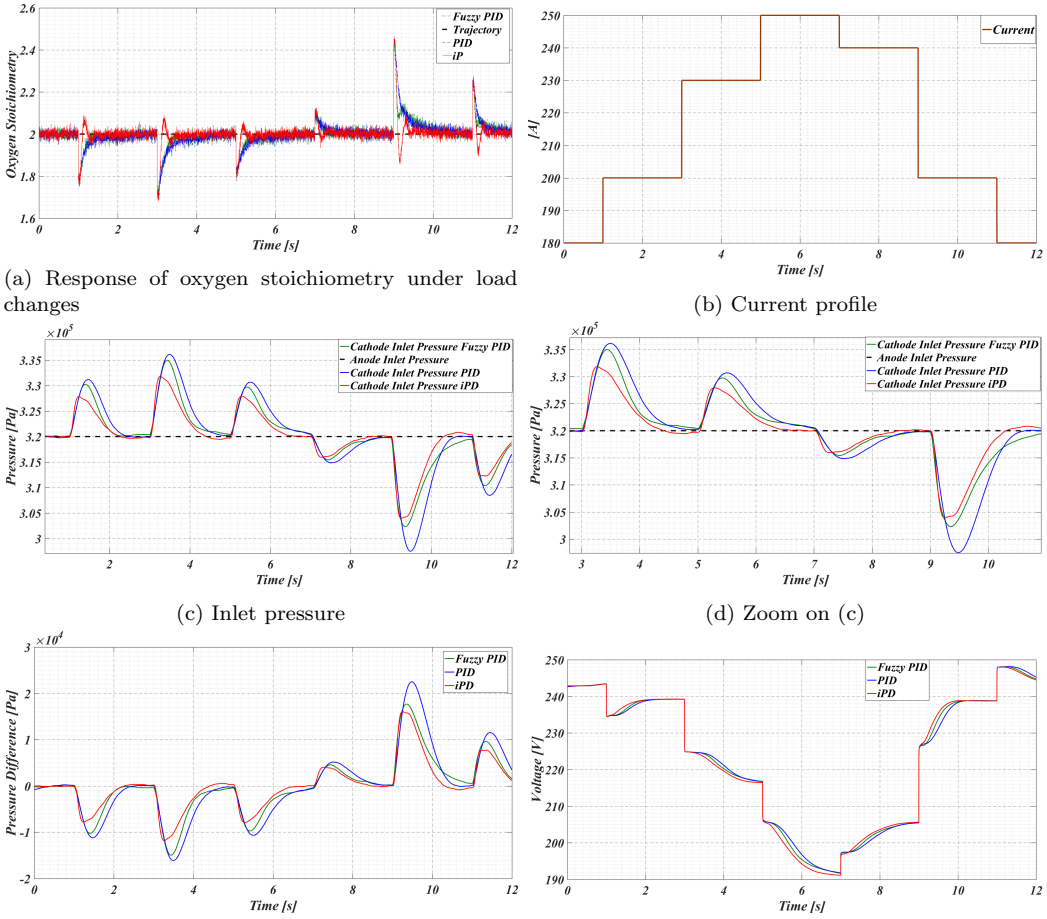

(a) Response of oxygen stoichiometry under load changes

(b) Current profile

(c) Inlet pressure

(d) Zoom on (c)

(e) Inlet difference pressure ΔP

(f) Voltage of PEM fuel cell

Figure 4: Disturbances rejection

3.3. Inlet pressure trajectory tracking

For this scenario, a variation of the hydrogen inlet pressure is performed. The objective is to ensure that the air pressure follows this variation to guarantee a zero pressure difference. The current and the oxygen stoichiometry are fixed at 180 A and 2 respectively. The pressure at the beginning is 2.5 barg, an increase of 0.5 barg of the hydrogen pressure is made at 0.8s. A decrease of 0.6 barg is made at 4s followed by an increase of 0.4 barg at 8s as shown in Fig5(a). For trajectory increment, the proposed controller provides faster trajectory tracking than fuzzy PID and PID. The latter provides overshoots during setpoint increments, see Fig5(b). The fact that the proposed controller is faster, translates into a slight difference in inlet diffrence pressure compared to other controllers as shown in Fig5(c). The pressure difference is

effectively guaranteed to be less than 0.1 barg with the proposed controller compared to others that exceed 0.2 barg for this scenario. It should be noted that this difference is significant in the real application where the interest of the proposed controller is to reduce the PEMFC pressure drop. Fig5(d) shows that the stoichiometry is kept 2 during inlet pressure changes. Since oxygen stoichiometry is correlated with noise, there is no significant difference between the controllers when the input pressures are changed, as shown in Fig5(d). Although, the iP controller is slightly faster than the others.

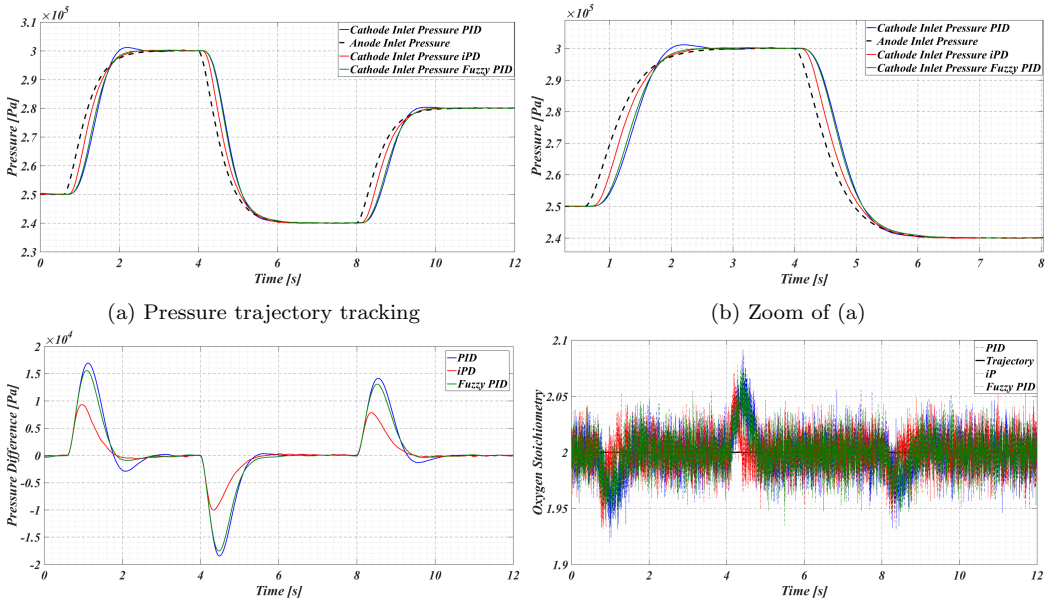

(a) Pressure trajectory tracking

(b) Zoom of (a)

(c) Inlet difference pressure ΔP

(d) Oxygen stoichiometry

Figure 5: Inlet pressure trajectory tracking with reducing the inlet pressure difference

To quantify the performance of controllers, four criteria are used: Integral Absolute Error $(IAE) = \int_0^t |e(t)|$, Integral of the Square Error $(ISE) = \int_0^t e(t)^2$, Integral of the Square input$(ISU) = \int_0^t u(t)^2$and Root Mean Square Error $(RMSE) = \sqrt{\frac{\sum_{i=1}^{N} e^2}{N}}$. The performance indexes Table 2 confirm that the iP and iPD controllers are considerably more efficient than the Fuzzy PID and conventional PID. For all the error criteria $IAE, ISE, RMSE$, the proposed controller provides good performance compared to the fuzzy PID controller which itself provides more performance compared to the conventional PID.

As mentioned earlier, the purpose of oxygen stoichiometry control is to avoid the

starvation fault that occurs if the fuel cell is exposed for a long time below a stoichiometry of 2. The simulation figures and performance tables show that the proposed controller performs much better than the Fuzzy PID and conventional PID. Rapid adjustment of oxygen stoichiometry under different current changes is noticed as well as an excellent trajectory tracking without overshoot. Regarding the control of the inlet pressure difference, the iPD controller provides less difference in the three cases studied in this part of the simulation. This prevents the occurrence of mechanical degradation of the membrane.

Index performance	IAE	ISE	ISU	RMSE
iP	0.15	0.014	1.53×10^2	0.0027
iPD	1.7×10^4	1.24×10^8	1.39	2.47×10^7
PID for oxygen stoichiometry	0.22	0.0217	1.52×10^2	0.004
PID for ΔP	2.7×10^4	2.6×10^8	1.4295	5.38×10^7
Fuzzy PID for oxygen stoichiometry	0.1854	0.0186	1.53×10^2	0.0032
Fuzzy PID for ΔP	2.1×10^4	1.82×10^8	1.42	3.53×10^7

Table 2: performance indexes

4. Experimental results :

4.1. Test bench description

The laboratory test bench where the experiments are performed is dedicated to PEM fuel cell stack that have a power lower than 1.5 Kw. The control and the measurement of flow mass are performed by a SLA5850 mass flow controller, manufactured by BROOKS instrument. The relative humidity of inlet gases is adjusted by setting the temperature of the humidification bottles and pre-heating channels. For both anode and cathode inlets, it gives access to the measurement of inlet pressure, temperature and relative humidity of the gases. Two back pressure valves (Kammer vannes) are located at the gas outlet of the stack. These valves allow to control the pressure of either the stack inlet or the outlet. The basic configuration for the pressure control of the test bench is done via two industrial PID controllers (West 5010), which ensure the pressure control of the stack. The temperature management of the stack is ensured with 3 elements: a pump that regulates the flow of water entering the stack, a heating channel to heat the water at the start of the tests and an exchanger that cools the water leaving the stack.

Fuel cell Temperature	Cooling flow rate	RH	Air stoichiometry	Hydrogen stoichiometry
$60°C$	$1l/min$	60%	2	2

Table 3: Operating condition of PEM fuel cell stack

The System Control and Data Acquisition (SCDA) is implemented through LabView, which allows setting different parameters of the PEMFC as well as adjusting the load. Indeed, the proposed control algorithm for the inlet pressure is implemented in Labview under NI PXI-1031, the manipulated variable is the voltage that controls the opening and closing of the back pressure valves. These are controlled by [4-20 mA] sent by the Ni daq board, 4 mA refers to the complete opening of the valve and 20 mA to the closing. The confidence interval of the sensors used for measuring the gas inlet pressure is ± 4 mbar. The sampling time is 3 Hz for the acquisition of the different data of the PEM fuel cell. It should be noted that oxygen stoichiometry control cannot be performed on the existing test bench architecture because the gases are supplied by cylinders, there is no compressor. Fig.6 shows the laboratory test bench where the tests are performed.

The stack where the experimental tests were performed contains 12 cells, with an active surface area of $90cm^2$ and rated power of 1.2 KW. The PEM fuel cell stack manufacturer specifies that the maximal ΔP, i.e the inlet difference pressure must not exceed 0.3 barg. The operating condition of PEM fuel cell stack are given in Table. 3.

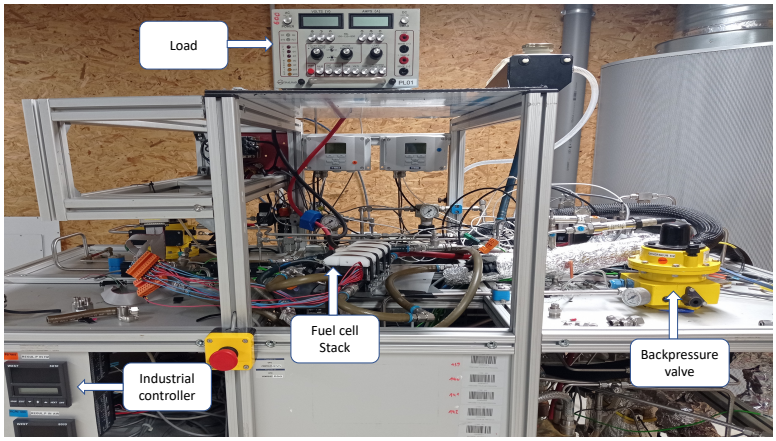

Figure 6: Laboratory test bench

The first objective of this experimental part is to validate the excellent performances

iPD controller for anode side	iPD controller for cathode side
$\alpha = 10; Kp = -30; Kd = -3$	$\alpha = 0.4; Kp = 0.1; Kd = 0.2$

Table 4: Gain values of the controllers

obtained in the previous section with the proposed controller in a real application. Moreover, the second objective is to compare its performances with the integrated controller on the test bench. The idea is to evaluate a possible replacement of the regulators on the test bench with the proposed approach. Since the model of the fuel cell stack and all the auxiliaries that make up the fuel cell system is unknown, it is very difficult to apply an model-based approaches. As, the computer performing the computations is equipped with a 2.0GhZ processor and 504 MB of RAM, the proposed approach is appropriate considering that it does not require a high computational time and was implemented without the need for a specific toolbox.
The controller gain values used in the experiment are given in Table 4.

4.2. Inlet pressure control stack

The pressure control strategy employed for this experimental section is as follows: follow the desired trajectory for the inlet pressure on the anode side. The hydrogen inlet pressure is assumed as the reference to be followed for the air inlet pressure. This strategy tests both the performance of the controllers in following the desired trajectory and the reduction of the input pressure difference. The control scheme of the adopted control strategy is illustrated in Fig.7.

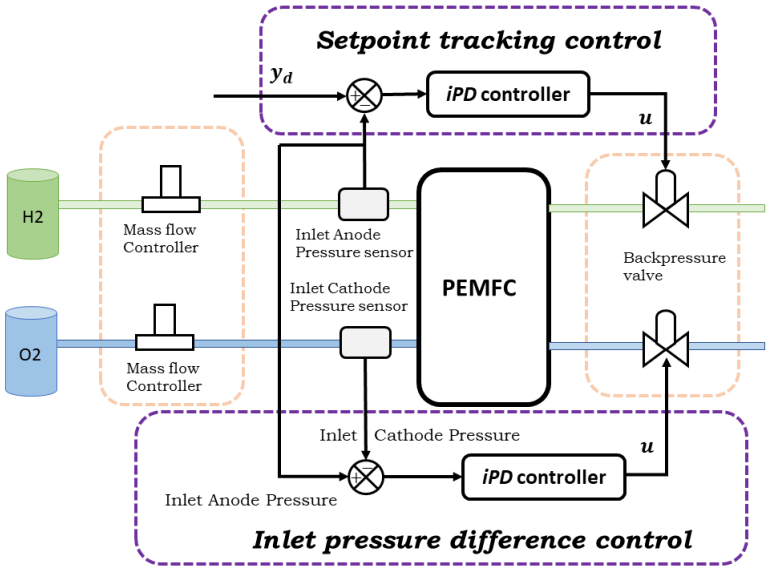

Figure 7: Pressure control scheme

4.2.1. Model free controller

Two case studies are performed: following the trajectory with a current fixed at 80 A, and varying the current in order to maintain the inlet pressure difference around 0. An ultra-local model of order 2 is taken for this experimental part, which implies the implementation of an iPD controller. In general, the design of the model-free controller starts with an model-ultra local of order 1, i.e., the iP controller. If the results obtained are not suitable, a model of order 2 is envisaged.

4.2.1.1. Setpoint tracking. The experiment for the different set point changes lasts 27 minutes. The desired trajectory is set to achieve the set point in 1 minute as illustrated in Fig.8(a). Fig.8(b) shows the potential of the proposed controller to quickly follow both trajectories. The first trajectory imposed by the user governing the inlet pressure on the anode side. The second trajectory is that of the hydrogen inlet pressure which is driving the air pressure, with no overshoot noted. The time taken for both inlet pressures to stabilize at the desired set point is about one minute. This stabilization time is defined by the desired trajectory, which makes the iPD Controller a very suitable tool for this application. At the beginning the inlet pressure is 1.4 , a large increase of 0.2 barg is made at 1.5 min, and a significant decrease of 0.3 barg is made at 7 min. As for the high set point changes and for the others that have a lower amplitude, the time to reach the desired set point is the same. This fast tracking results in a reduction of the inlet pressure difference, which is the

objective of this control strategy as shown in Fig.8(c). In this entire experiment, the highest ΔP recorded is 20 mbar which is far below the stack manufacturer's recommendations for inlet pressure difference, that is, 0.3 barg. The stack voltage signal also shows that a quick adjustment of the input pressure has a direct impact on the performance. The voltage signal climbs rapidly when increasing the inlet pressure for both sides of the stack, see Fig.8(d).

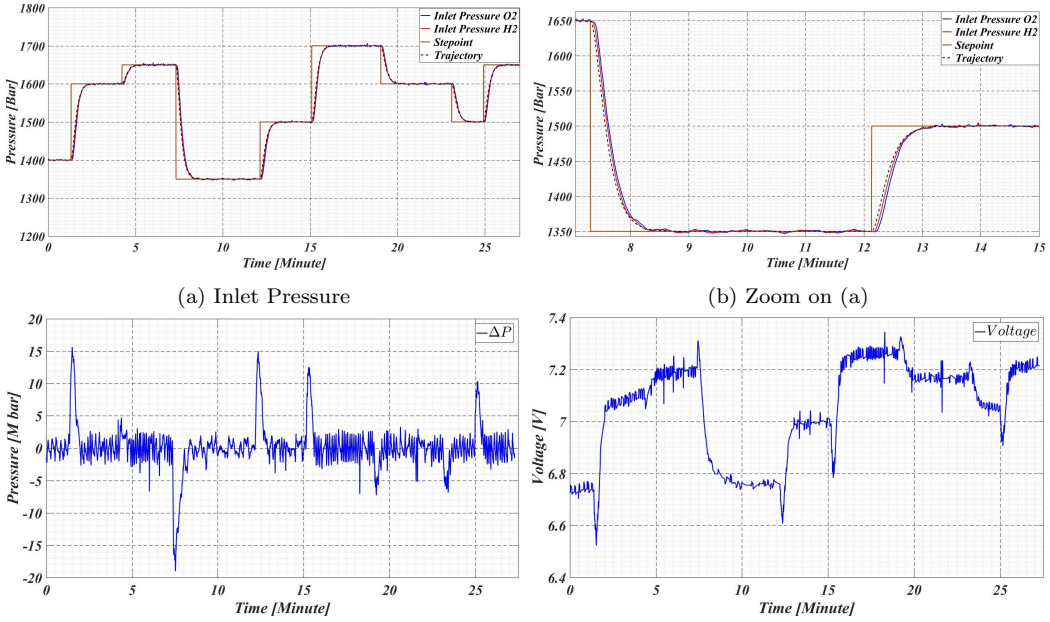

(a) Inlet Pressure

(b) Zoom on (a)

(c) ΔP

(d) Voltage

Figure 8: Setpoint tracking with model-free controller

4.2.1.2. Current variation. The inlet pressure for both sides is regulated to maintain 1.65 barg for different variation of the current. In general, both inlet pressures are adjusted to the desired set point in 1 min for the biggest variation of current and less than 1 min for the lower variation as shown in Fig.9(a). The current variation profile is illustrated in Fig.9(b). The inlet pressure difference is maintained around 0 quickly for all the current variation as shown in Fig.9(c). The fluctuation of +/- 4 mbarg is noticed which is linked to the noise of the sensor. As the variation of the current induced the change of the flow rate of the gases, the Fig.9(d) shows the inlet mass flow rate for both anode and cathode sides. Proper pressure control results in a steady voltage signal of the stack as shown in Fig.9(e).

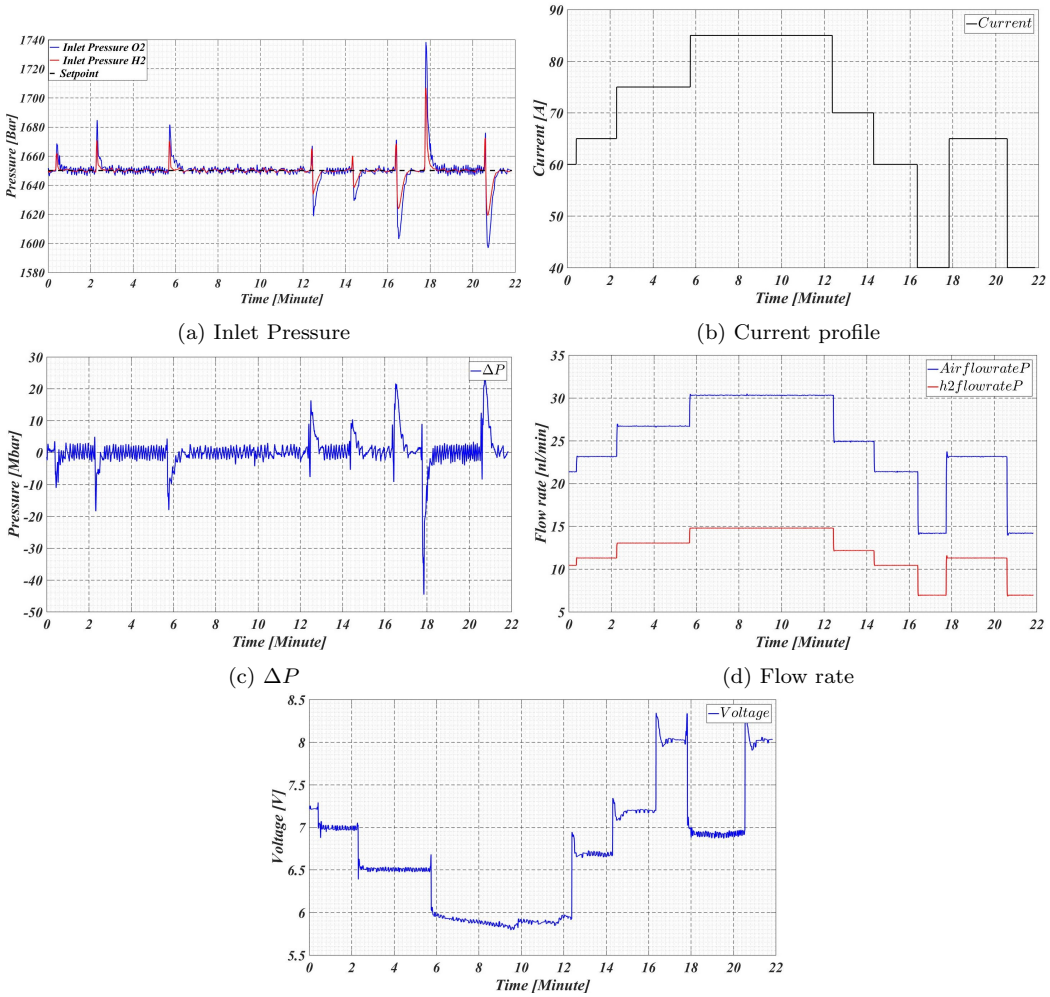

(a) Inlet Pressure

(b) Current profile

(c) ΔP

(d) Flow rate

(e) Stack voltage

Figure 9: Current variation with model-free controller

4.2.2. Test bench controller

The integrated controller of the test bench is an industrial PID controller. The configuration chosen for the pressure control is that the desired setpoint governs the air inlet pressure. This is used as a reference for the hydrogen pressure control. In general, this is the opposite of the architecture proposed above. It should be noted that this configuration can in no way influence the quality of the control.

4.2.2.1. Setpoint tracking. The setpoint changes profile is the same as before, but with a longer time span of 43 min. This can be explained by the fact that the

controller takes a long time to reach the desired setpoint as shown in Fig.10(a). For the first setpoint change up to 1.6 barg, the air inlet pressure takes 2 minutes to reach the setpoint while the hydrogen inlet pressure takes about 2.5 minutes. In the event of a setpoint decrease from 1.65 barg to 1.35 barg, a time of approximately 4 minutes is noted, see Fig.10(b). This time is too slow compared to the proposed controller. For other small amplitude changes, the stabilization time for both inlet pressures is approximately 2.5 min. The inlet pressure difference ΔP is illustrated in Fig.10(c) for this setpoint change profile. The ΔP signal emphasizes that poor inlet pressure control can result in up to 100 mbarg of inlet pressure difference. This represents 5 times larger than the proposed controller for the same scenario. For small amplitude variations, this difference is less than 50 mbarg, which is acceptable but it takes a little longer to reach the desired set point. The stack voltage signal in Fig.10(d). The voltage evolution follows the pressure profiles but slightly slower than the iPD controller.

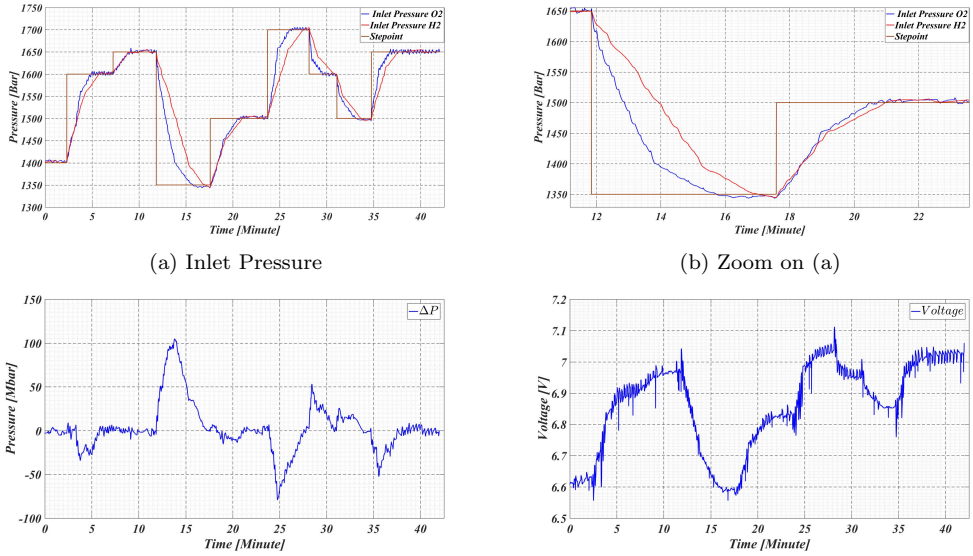

(a) Inlet Pressure

(b) Zoom on (a)

(c) ΔP

(d) Voltage

Figure 10: Setpoint tracking with test bench controller

4.2.2.2. Current variation. The controller integrated in the test bench is also tested under load variation, see Fig.11(a). The same profile as before is applied with the same control objective. Fig.11(b) shows the inlet pressure of anode and cathode sides for this scenario. It can be noticed that there are two distinct behaviors of the controller: the first is when the current increases, the pressure difference is

maintained at about 0 quickly. In case the current decreases, it behaves very slowly. It takes more time, around 1.5 min to reach the set point of ΔP which is 0, see Fig.11(c). For the last current decrease which is 25 A, the controller needs more than 2 min to stabilize the pressure difference around 0. This is regarded as slow compared to the iPD controller which ensures the stabilization of ΔP in less than one minute for all the investigated scenarios. The inlet gas flow for this experiment is shown in the Fig.11(d) which allows to ensure the required stoichiometry. The stack voltage is shown in Fig.10(e). A slight decrease in performance on this test scenario is noted on this voltage signal compared to the proposed controller.

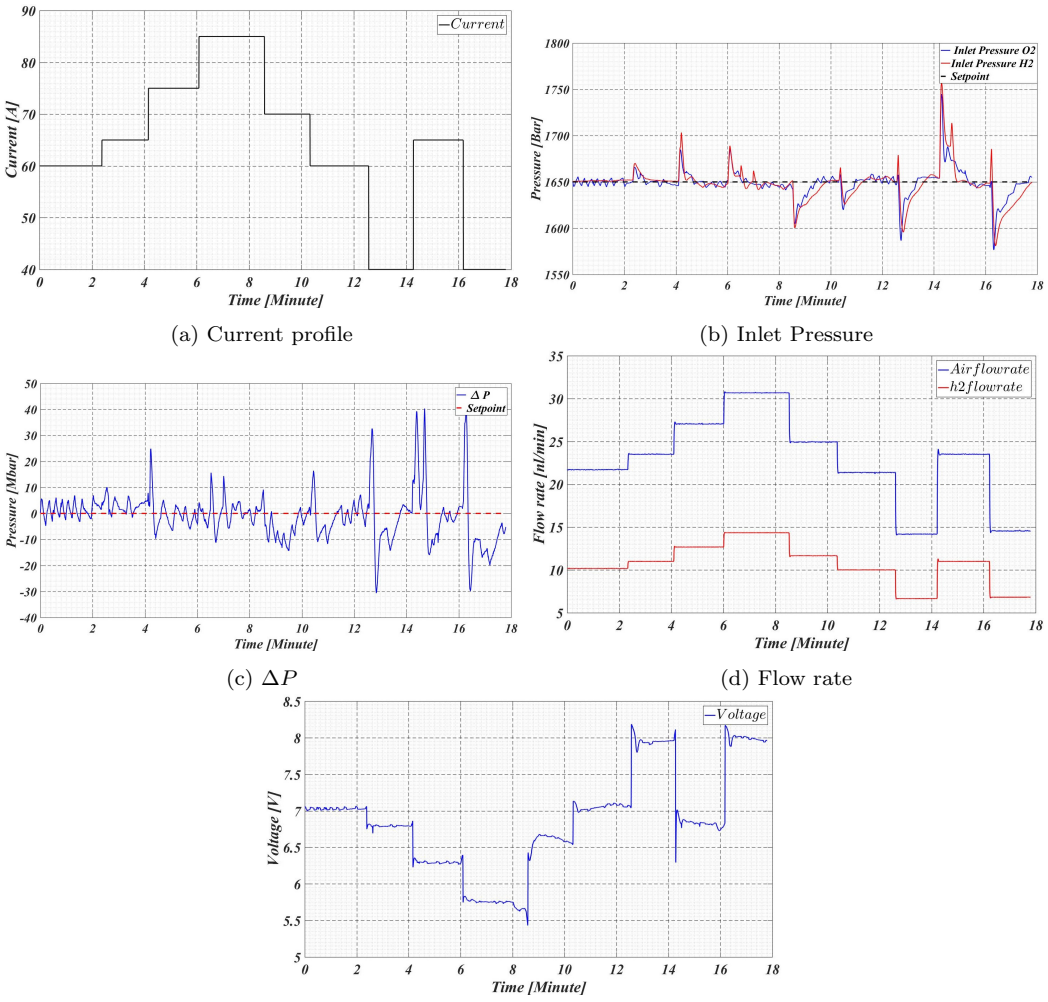

(a) Current profile

(b) Inlet Pressure

(c) ΔP

(d) Flow rate

(e) Stack voltage

Figure 11: Current variation with test bench controller

The proposed controller confirmed that it guarantees less pressure input differential for the two cases studied compared to the test bench controller. For the first scenario studied, the proposed controller reaches the desired setpoint twice as fast as the controller integrated on the test bench. In addition, for some scenarios studied, it ensures an inlet pressure difference 5 times lower than that the tests bench controller. This eliminates the risk of degradation on the membrane that is related to the inlet pressure, which is not the case with the integrated controller. The satisfactory experimental results obtained, encouraged us to replace the pressure control strategy of the test bench with the proposed controller. This choice was supported by the fact that there is no need to add any necessary equipment and the fact of having a low computational cost with no precious knowledge of the fuel cell model. This is perfectly suitable for stack pressure control in a real application.

5. Conclusion and perspectives

In this work, a model free (iP) and (iPD) controllers are introduced to control both oxygen stoichiometry and pressure difference of PEM fuel cell. The main benefit of the model-free control approach is that it does not require an accurate model of the PEMFC system. Obtaining the model is often a complicated task due to the coupling of electrical, thermal and fluidic phenomena. In a first step, the oxygen stoichiometry control and inlet pressure differnce are performed in simulation using a nonlinear model. A comprehensive comparison with a Fuzzy PID and PID controller is performed in order to evaluate the performance of the proposed controller. The proposed controller showed excellent ability to restore oxygen stoichiometry and air inlet pressure when the current changes, and to reach the desired trajectory very quickly without any overshoot. The assessment of controller performance is done using performance indexes IAE, ISE, ISU and $RMSE$ for simulation part. The proposed controller exhibits good efficiency compared to the Fuzzy PID and PID controller. In the second step, a control of inlet pressure difference is applied for a $1.2KW$ stack in experimentation. The proposed controller showed successful tracking of hydrogen inlet pressure variations, and ensured an inlet difference pressure less than 50 mbarg for all cases studied. By limiting a large depression difference, perforation of the membrane is avoided and the health of the fuel cell is preserved. Overall, it is twice as fast at following the set point as the test bench controller and provides 5 times less input pressure difference for the first scenario studied in the experimental part. We emphasize that the model free controller is inexpensive in computation time and implementation complexity for online control compared to other approaches.

In the future, the proposed method will be tested for controlling stack temperature and inlet relative humidity. The second future objective is to integrate the controller into the fault tolerant control strategy block with online fault detection to ensure stack durability.

Acknowledgments This project has received funding from the Reunion Island Region under grant number and the European Commission - European Regional Development Fund (ERDF) –Operational Programme 2014-2020. This work has been supported by the EIPHI Graduate school (contract "ANR-17-EURE-0002").

References

[1] H. Askaripour, Effect of operating conditions on the performance of a PEM fuel cell, International Journal of Heat and Mass Transfer 144 (2019) 118705. URL: https://linkinghub.elsevier.com/retrieve/pii/S0017931019328467. doi:10.1016/j.ijheatmasstransfer.2019.118705.

[2] W. Schmittinger, A. Vahidi, A review of the main parameters influencing long-term performance and durability of PEM fuel cells, Journal of Power Sources 180 (2008) 1–14. URL: https://linkinghub.elsevier.com/retrieve/pii/S0378775308001924. doi:10.1016/j.jpowsour.2008.01.070.

[3] P. Pei, H. Chen, Main factors affecting the lifetime of Proton Exchange Membrane fuel cells in vehicle applications: A review, Applied Energy 125 (2014) 60–75. URL: https://linkinghub.elsevier.com/retrieve/pii/S0306261914002797. doi:10.1016/j.apenergy.2014.03.048.

[4] N. Yousfi-Steiner, P. Moçotéguy, D. Candusso, D. Hissel, A. Hernandez, A. Aslanides, A review on PEM voltage degradation associated with water management: Impacts, influent factors and characterization, Journal of Power Sources 183 (2008) 260–274. URL: https://linkinghub.elsevier.com/retrieve/pii/S0378775308007337. doi:10.1016/j.jpowsour.2008.04.037.

[5] R. Petrone, Z. Zheng, D. Hissel, M.-C. Péra, C. Pianese, M. Sorrentino, M. Becherif, N. Yousfi-Steiner, A review on model-based diagnosis methodologies for pemfcs, International Journal of Hydrogen Energy 38 (2013) 7077–7091.

[6] L. Yin, Q. Li, T. Wang, L. Liu, W. Chen, Real-time thermal Management of Open-Cathode PEMFC system based on maximum efficiency control strategy, Asian Journal of Control 21 (2019) 1796–1810. URL: https://onlinelibrary.wiley.com/doi/abs/10.1002/asjc.2207. doi:10.1002/asjc.2207.

[7] S. Chugh, C. Chaudhari, K. Sonkar, A. Sharma, G. Kapur, S. Ramakumar, Experimental and modelling studies of low temperature PEMFC performance, International Journal of Hydrogen Energy 45 (2020) 8866–8874. URL: https://linkinghub.elsevier.com/retrieve/pii/S036031992030077X. doi:10.1016/j.ijhydene.2020.01.019.

[8] H. Choi, J. Kim, O. Kwon, H. Yoo, H. Kim, H. Cha, T. Park, Observation of flooding-induced performance enhancement in pemfcs, International Journal of Hydrogen Energy 47 (2022) 6259–6268.

[9] S. Kim, I. Hong, Effects of humidity and temperature on a proton exchange membrane fuel cell (PEMFC) stack, Journal of Industrial and Engineering Chemistry 14 (2008) 357–364. URL: https://linkinghub.elsevier.com/retrieve/pii/S1226086X08000142. doi:10.1016/j.jiec.2008.01.007.

[10] S. Raman, S. Swaminathan, S. Bhardwaj, H. K. Tanneru, B. Bullecks, R. Rengaswamy, Rapid humidity regulation by mixing of dry and humid gases with feedback control for PEM fuel cells, International Journal of Hydrogen Energy 44 (2019) 389–407. URL: https://linkinghub.elsevier.com/retrieve/pii/S0360319918314046. doi:10.1016/j.ijhydene.2018.04.187.

[11] J. Chen, Z. Liu, F. Wang, Q. Ouyang, H. Su, Optimal Oxygen Excess Ratio Control for PEM Fuel Cells, IEEE Transactions on Control Systems Technology 26 (2018) 1711–1721. URL: https://ieeexplore.ieee.org/document/7987780/. doi:10.1109/TCST.2017.2723343.

[12] Y. Zhu, J. Zou, S. Li, C. Peng, An adaptive sliding mode observer based near-optimal oer tracking control approach for pemfc under dynamic operation condition, International Journal of Hydrogen Energy 47 (2022) 1157–1171.

[13] M. Li, J. Lu, Y. Hu, J. Gao, Oxygen Excess Ratio Controller Design of PEM Fuel Cell, IFAC-PapersOnLine 51 (2018) 493–498. URL: https://linkinghub.elsevier.com/retrieve/pii/S2405896318325722. doi:10.1016/j.ifacol.2018.10.108.

[14] Y. Ma, F. Zhang, J. Gao, H. Chen, T. Shen, Oxygen excess ratio control of PEM fuel cells using observer-based nonlinear triple-step controller, International Journal of Hydrogen Energy (2019) S0360319919338777. URL: https://linkinghub.elsevier.com/retrieve/pii/S0360319919338777. doi:10.1016/j.ijhydene.2019.10.089.

[15] L. Sun, J. Shen, Q. Hua, K. Y. Lee, Data-driven oxygen excess ratio control for proton exchange membrane fuel cell, Applied Energy 231 (2018) 866–875. URL: https://linkinghub.elsevier.com/retrieve/pii/S0306261918313448. doi:10.1016/j.apenergy.2018.09.036.

[16] F. Chen, Y. Yu, Y. Gao, Temperature Control for Proton Exchange Membrane Fuel Cell based on Current Constraint with Consideration of Limited Cooling Capacity, Fuel Cells 17 (2017) 662–670. URL: http://doi.wiley.com/10.1002/fuce.201700001. doi:10.1002/fuce.201700001.

[17] L. Huang, J. Chen, Z. Liu, M. Becherif, Adaptive thermal control for pemfc systems with guaranteed performance, International Journal of Hydrogen Energy 43 (2018) 11550–11558.

[18] C. Damour, M. Benne, B. Grondin-Perez, J.-P. Chabriat, B. G. Pollet, A novel non-linear model-based control strategy to improve pemfc water management–the flatness-based approach, international journal of hydrogen energy 40 (2015) 2371–2376.

[19] M. Solsona, C. Kunusch, C. Ocampo-Martinez, Control-oriented model of a membrane humidifier for fuel cell applications, Energy Conversion and Management 137 (2017) 121–129. URL: https://linkinghub.elsevier.com/retrieve/pii/S0196890417300444. doi:10.1016/j.enconman.2017.01.036.

[20] H. Deng, Q. Li, Y. Cui, Y. Zhu, W. Chen, Nonlinear controller design based on cascade adaptive sliding mode control for PEM fuel cell air supply systems, International Journal of Hydrogen Energy 44 (2019) 19357–19369. URL: https://linkinghub.elsevier.com/retrieve/pii/S0360319918334438. doi:10.1016/j.ijhydene.2018.10.180.

[21] C. Damour, M. Benne, C. Lebreton, J. Deseure, B. Grondin-Perez, Real-time implementation of a neural model-based self-tuning PID strategy for oxygen stoichiometry control in PEM fuel cell, International Journal of Hydrogen Energy 39 (2014) 12819–12825. URL: https://linkinghub.elsevier.com/retrieve/pii/S0360319914016802. doi:10.1016/j.ijhydene.2014.06.039.

[22] J. Chen, W. Yao, Q. Lu, X. Duan, B. Yang, F. Zhu, X. Cao, L. Jiang, Robust nonlinear adaptive pressure control of polymer electrolyte membrane fuel cells considering sensor failures based on perturbation compensation, Energy Reports 8 (2022) 8396–8412.

[23] E. Mohammed Ali et. al., Pressure Regulation in Proton Exchange Membrane Fuel Cell using Direct Active Fuzzy Non-Linear Controller, International Journal of Computing and Digital Systems 9 (2020) 61–68. URL: https://journal.uob.edu.bh/handle/123456789/3698. doi:10.12785/ijcds/090106.

[24] J. Chen, C. Zhang, K. Li, Y. Zhan, B. Sun, Hybrid adaptive control for pemfc gas pressure, Energies 13 (2020) 5334.

[25] H. Yuan, H. Dai, W. Wu, J. Xie, J. Shen, X. Wei, A fuzzy logic pi control with feedforward compensation for hydrogen pressure in vehicular fuel cell system, International Journal of Hydrogen Energy 46 (2021) 5714–5728.

[26] H. Zhang, Y. Wang, D. Wang, Y. Wang, Adaptive robust control of oxygen excess ratio for PEMFC system based on type-2 fuzzy logic system, Information Sciences 511 (2020) 1–17. URL: https://linkinghub.elsevier.com/retrieve/pii/S0020025519307315. doi:10.1016/j.ins.2019.08.005.

[27] W.-J. Zou, Y.-B. Kim, Temperature Control for a 5 kW Water-Cooled PEM Fuel Cell System for a Household Application, IEEE Access 7 (2019) 144826–144835. URL: https://ieeexplore.ieee.org/document/8861321/. doi:10.1109/ACCESS.2019.2945986.

[28] M. S. AbouOmar, Y.-X. Su, H.-J. Zhang, Hybrid Feedback-Feedforward Fuzzy Control of PEM Fuel Cell Air Feed System with Electromagnetic Field Optimization, IETE Journal of Research (2019) 1–17. URL: https://www.tandfonline.com/doi/full/10.1080/03772063.2019.1617199. doi:10.1080/03772063.2019.1617199.

[29] Z. Fan, X. Yu, M. Yan, C. Hong, Oxygen Excess Ratio Control of PEM Fuel Cell Based on Self-adaptive Fuzzy PID, IFAC-PapersOnLine 51 (2018) 15–20. URL: https://linkinghub.elsevier.com/retrieve/pii/S2405896318324650. doi:10.1016/j.ifacol.2018.10.004.

[30] M. Fliess, C. Join, Model-free control, International Journal of Control 86 (2013) 2228–2252. URL: http://www.tandfonline.com/doi/abs/10.1080/00207179.2013.810345. doi:10.1080/00207179.2013.810345.

[31] C. Join, F. Chaxel, M. Fliess, "intelligent" controllers on cheap and small programmable devices, in: 2013 Conference on Control and Fault-Tolerant Systems (SysTol), IEEE, 2013, pp. 554–559.

[32] P. Polack, S. Delprat, B. d'Andréa Novel, Brake and velocity model-free control on an actual vehicle, Control Engineering Practice 92 (2019) 104072. URL: https://linkinghub.elsevier.com/retrieve/pii/S0967066119300851. doi:10.1016/j.conengprac.2019.06.011.

[33] F. Lafont, J.-F. Balmat, N. Pessel, M. Fliess, A model-free control strategy for an experimental greenhouse with an application to fault accommodation, Computers and Electronics in Agriculture 110 (2015) 139–149. URL: https://linkinghub.elsevier.com/retrieve/pii/S0168169914002890. doi:10.1016/j.compag.2014.11.008.

[34] C. Join, J. Bernier, S. Mottelet, M. Fliess, S. Rechdaoui-Guérin, S. Azimi, V. Rocher, A simple and efficient feedback control strategy for wastewater denitrification, IFAC-PapersOnLine 50 (2017) 7657–7662. URL: https://linkinghub.elsevier.com/retrieve/pii/S2405896317316622. doi:10.1016/j.ifacol.2017.08.1167.

[35] O. Bara, M. Fliess, C. Join, J. Day, S. M. Djouadi, Toward a model-free feedback control synthesis for treating acute inflammation, Journal of Theoretical Biology 448 (2018) 26–37. URL: https://linkinghub.elsevier.com/retrieve/pii/S0022519318301632. doi:10.1016/j.jtbi.2018.04.003.

[36] J. M. Barth, J.-P. Condomines, M. Bronz, J.-M. Moschetta, C. Join, M. Fliess, Model-free control algorithms for micro air vehicles with transitioning flight capabilities, International Journal of Micro Air Vehicles 12 (2020) 1756829320914264. URL: https://doi.org/10.1177/1756829320914264. doi:10.1177/1756829320914264. arXiv:https://doi.org/10.1177/1756829320914264.

[37] L. Menhour, B. d'Andréa Novel, M. Fliess, D. Gruyer, H. Mounier, An efficient model-free setting for longitudinal and lateral vehicle control. Validation through the interconnected pro-SiVIC/RTMaps prototyping platform, arXiv:1705.03216 [cs, math] (2017). URL: http://arxiv.org/abs/1705.03216, arXiv: 1705.03216.

[38] M. Fliess, H. Sira-Ramírez, Closed-loop Parametric Identification for Continuous-time Linear Systems via New Algebraic Techniques, in: M. J. Grimble, M. A. Johnson, H. Garnier, L. Wang (Eds.), Identification of Continuous-time Models from Sampled Data, Springer London, London, 2008, pp. 363–391. URL: http://link.springer.com/10.1007/978-1-84800-161-9_13. doi:10.1007/978-1-84800-161-9_13, series Title: Advances in Industrial Control.

[39] M. Mboup, C. Join, M. Fliess, Numerical differentiation with annihilators in noisy environment, Numerical Algorithms 50 (2009) 439–467. URL: http://link.springer.com/10.1007/s11075-008-9236-1. doi:10.1007/s11075-008-9236-1.

[40] M. Fliess, R. Marquez, Continuous-time linear predictive control and flatness: A module-theoretic setting with examples, International Journal of Control 73 (2000) 606–623. URL: https://doi.org/10.1080/002071700219452. doi:10.1080/002071700219452. arXiv:https://doi.org/10.1080/002071700219452.

[41] J. T. Pukrushpan, A. G. Stefanopoulou, H. Peng, Modeling and control for pem fuel cell stack system, in: Proceedings of the 2002 American Control Conference (IEEE Cat. No. CH37301), volume 4, IEEE, 2002, pp. 3117–3122.

[42] Z. Baroud, A. Benalia, C. Ocampo-Martinez, Robust fuzzy sliding mode control for air supply on pem fuel cell system, International Journal of Modelling, Identification and Control 29 (2018) 341–351.

[43] R. Da Fonseca, E. Bideaux, M. Gerard, B. Jeanneret, M. Desbois-Renaudin, A. Sari, Control of pemfc system air group using differential flatness approach: Validation by a dynamic fuel cell system model, Applied energy 113 (2014) 219–229.

[44] P. Meshram, R. G. Kanojiya, Tuning of pid controller using ziegler-nichols method for speed control of dc motor, in: IEEE-international conference on advances in engineering, science and management (ICAESM-2012), IEEE, 2012, pp. 117–122.

[45] Z. Baroud, M. Benmiloud, A. Benalia, C. Ocampo-Martinez, Novel hybrid fuzzy-pid control scheme for air supply in pem fuel-cell-based systems, International Journal of Hydrogen Energy 42 (2017) 10435–10447.